

PAPER • OPEN ACCESS

Roughness Prediction Model of Face Milling Surface for Nickel-Based Superalloy FGH97

To cite this article: Yang Qiao *et al* 2019 *IOP Conf. Ser.: Mater. Sci. Eng.* **562** 012154

View the [article online](#) for updates and enhancements.

You may also like

- [Fast gas heating of nanosecond pulsed surface dielectric barrier discharge: spatial distribution and fractional contribution from kinetics](#)
Yifei Zhu and Svetlana Starikovskaia
- [Ultrathin Ru-Ta-C Barriers for Cu Metallization](#)
J. S. Fang, J. H. Lin, B. Y. Chen *et al.*
- [Effect of solution treatment temperature on the precipitation distribution, high temperature tensile and fatigue properties of FGH96 joints prepared by inertia friction welding](#)
Jun Yang, Jinglong Li, Jiangtao Xiong *et al.*



ECS
The
Electrochemical
Society
Advancing solid state &
electrochemical science & technology

DISCOVER
how sustainability
intersects with
electrochemistry & solid
state science research

Roughness Prediction Model of Face Milling Surface for Nickel-Based Superalloy FGH97

Yang Qiao, Peiquan Guo*, Hongtang Chen, Shouren Wang and Tonghui Liu

Department of Mechanical Engineering, University of Jinan, 336 Nanxinzhuanxi Road, Jinan, Shandong 250022, P.R. China.

Email: oss_guopq@ujn.edu.cn

Abstract. An experimental investigation based on the Taguchi orthogonal array was conducted to analyze the effects of cutting parameters on machined surface roughness Ra for nickel-based superalloy FGH97. The influence order and significance of processing parameters that affect Ra were determined according to variance analysis. Machined surface roughness prediction model has been constructed based on experimental results. Cutting speed has the greatest influence on the surface roughness of the workpiece. The effect of depth of cut on the surface roughness is not obvious, but the surface roughness will be larger when the depth of cut exceeds 0.20 mm. The effect of width of cut on machined surface roughness is negligible.

1. Introduction

Powder superalloys are a kind of materials with excellent mechanical properties, thermal properties, thermal fatigue properties. They are the most suitable materials for the key parts of modern aeroengine, ship gas turbine, rocket engine and nuclear reactor. In the early 1970s, the P&WA Company of the United States of America developed powder superalloy IN100, which is used for engine turbine discs of fighter airplane F15 and F16. GE developed René88DT turbine disc by argon atomization and hot extrusion and isothermal forging in 1988. The turbine disc is widely used in civil and military aircraft [1,2]. In the 1990s, the United States has developed the third generation powder superalloys, such as Alloy10, René104 and RR1000 [3,4]. Superalloy FGH95, FGH96 and FGH97 alloys have been developed successively after the late 1970s in China. Superalloy FGH95 is characterized as high strength at working temperature of 650 degrees Centigrade. Superalloy FGH96 can be used at temperatures up to 700-750 degrees Centigrade. It is a key material for preparing high performance engine turbine disk. Superalloy FGH97 prepared by plasma rotating electrode pulverizing and hot isostatic pressing has the advantages of high tensile strength and high creep resistance, and its crack propagation rate is one order of magnitude lower than that of FGH95 or FGH96 [5-7].

Currently, there is some research on machining of nickel-based superalloy. The effect of cutting parameters on cutting forces or wear and the characteristics of tool wear as machining Inconel 718 wear have been investigated [8, 9]. M.C. Hardy [10] reviewed techniques for inspecting the effects of process parameters on surface integrity for hole making and finish turning and then presents the findings of work that has been conducted to understand the influence of machining anomalies on fatigue life. Surface integrity of machined titanium alloy and nickel-based superalloy have been researched [11-13]. For example, A. Ginting et al investigated roughness, lay, defects, microhardness and microstructure alterations of titanium alloy under the dry milling process. J. Liu et al investigated roughness, residual stress, nanohardness of TB6 titanium alloy (Ti-10V-2Fe-3Al) after dry milling with carbide end mills. N Varote et al established the correlations between microstructure and surface integrity. machining induced residual stresses in turning of titanium and nickel based alloy have been



investigated [13-16]. For instance, Arranola et al researched machining induced residual stresses and predictions with 3-D Finite Element (FE) based simulations for nickel-based alloy IN718.

This study focused the influence order along with significance of processing parameters (cutting speed, feed rate, depth and width of cutting) on surface roughness when face milling FGH97 under dry machining condition and construct the prediction models for roughness R_a (average of absolute roughness) based on experimental results. Taguchi orthogonal design method and ANOVA were used in the analyses.

2. FGH97 Milling Test

2.1. Properties of FGH97

The composition of FGH97 is shown in Table 1. The alloy elements dissolve a large number of solid solutions in Co and Ni, i.e. the strengthening phase γ' . In order to ensure good strengthening effect, the content of strengthening phase γ' in FGH97 is about 64% of the alloy mass fraction. Its tensile strength is 1510 MPa, yield strength is 1080 MPa and solid solution temperature is 1180-1190 degrees Centigrade. Therefore, the physical properties of FGH97 seriously restrict its machinability. Because of the special manufacturing process of materials, thermal-induced pores are formed in the material during the manufacturing process. When the tool cuts the induced pores, the tool will be impacted. The continuous impact has a great impact on the tool performance. Moreover, the existence of thermal-induced pores is not conducive to the heat dissipation during the cutting process. The thermal induced porosity also severely restricts the machinability of the material. So, FGH97 is very difficult to be machined.

Table 1. Composition of FGH97 (wt%).

C	Cr	Co	Al	Ti	W	Nb	Hf	B	Zr	Mg	Ce	Ni
0.04	9.0	15.5	4.9	1.8	5.5	2.6	0.3	≤0.015	≤0.015	≤0.02	≤0.01	bal

2.2. Experiment and Test Setting

Milling experiments have been carried by means of a machining center YCM-V116B as shown in Figure 1. TiAlN-TiN coated carbide insert SECO made SEEX1204AFTN-MD18 is used to mill FGH97. Mill cutter consists of a cutter head R220.53-0050-12-4A and inserts mentioned above. Inserts are fixed on cutter head. cutter's geometric parameters are rake angle of 10° , clearance angle of 12° , cutting edge angle of 30° , distortion angle of 3° , tool cutting edge inclination angle of -10° . The value setting of cutting speed, feed rate, depth and width of cutting are shown in Table 2.

Table 2. Cutting parameters.

Factor	Level			
	1	2	3	4
Cutting speed v_c (m/min)	30	50	70	90
Feed per teeth f_z (mm/z)	0.05	0.10	0.15	0.20
Depth of cut a_p (mm)	0.10	0.15	0.20	0.25
Width of cut a_w (mm)	10	15	20	25

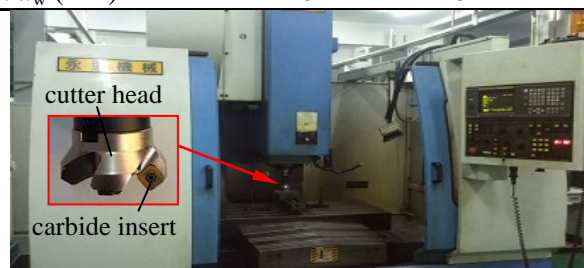


Figure 1. Machining center and cutter.

3. Test Results and Discussion

3.1. Test Results

The combinations of cutting speed, feed rate, depth and width of cutting are generated using an $L_{16}(4^5)$ orthogonal array as shown in Table 3. Surface roughness R_a (the arithmetic average of absolute roughness) of the machined surface were measured with surface roughness meter Mitutoyo SJ-410. And the measured values given in Table 3 were determined from the average values of five measurements to assure the reliability.

Table 3. Combination of variables and test results.

No.	v_c (m/min)	f_z (mm/z)	a_p (mm)	a_w (mm)	R_a (μm)
1	30	0.05	0.10	10	0.086
2	30	0.10	0.15	15	0.105
3	30	0.15	0.20	20	0.127
4	30	0.20	0.25	25	0.145
5	50	0.05	0.15	15	0.133
6	50	0.10	0.10	25	0.172
7	50	0.15	0.25	10	0.194
8	50	0.20	0.20	20	0.223
9	70	0.05	0.15	25	0.101
10	70	0.10	0.25	15	0.149
11	70	0.15	0.10	20	0.203
12	70	0.20	0.20	10	0.276
13	90	0.05	0.25	15	0.149
14	90	0.10	0.15	10	0.283
15	90	0.15	0.20	25	0.377
16	90	0.20	0.10	20	0.319

3.2. Test Result Analysis and Discussion

When the cutting parameters such as feed rate, depth of cut and width of cut remain unchanged, cutting speed is 30m/min, 50m/min, 70m/min or 90m/min, the corresponding machined surface roughness of the specimen as shown in Figure 2. Figure 2 shows that the surface roughness of Ni-based superalloy increases slowly with the increase of cutting speed when the cutting speed is 30-70 m/min. The main reason is that with the increase of cutting speed, the cutting force decreases, the extrusion force between the tool and the workpiece decreases, the plastic deformation degree in the deformation zone decreases, and the surface roughness decreases. In addition, with the increase of cutting speed, the heat generated by cutting decreases. When the heat accumulates to a certain extent, the friction coefficient decreases obviously due to the softening of the metal and the surface roughness decreases; and because the diameter of the cutter head used in this experiment is larger than 50 mm, when the cutting speed increases, the centrifugal force of the whole cutter becomes larger, resulting in the vibration of the whole cutter system is also increased, which will lead to the decrease of the surface roughness. The surface roughness of workpiece increases. Considering the influence of cutting force and tool vibration on the surface roughness of workpiece, the increase of surface roughness of workpiece is small and the change is not obvious. With the increase of cutting speed, when the cutting speed exceeds 70 m/min, the surface roughness of the workpiece increases rapidly. The reason is that the cutting speed is 90m/min and the cutting speed is too high. During the experiment, the tool appears to be overheated and reddened, which eventually leads to tool breakage and surface roughness of the workpiece increases rapidly. The reason for tool breakage is that for nickel-based powder metallurgy superalloys, cutting speed is 90 m/min, which is already a high-speed cutting. Under the condition of high-speed cutting, both the cutting tool and the workpiece bear very large cutting force and cutting heat. In the subsequent continuous machining process, excessive cutting speed eventually leads to tool collapse. Therefore, when cutting nickel base superalloy FGH97, the suitable cutting speed is about

50m/min. Figure 3 shows machined surface roughness corresponding to feed per tooth of 0.05mm/z, 0.10mm/z, 0.15mm/z, 0.20mm/z as cutting speed, depth of cut and width of cut remaining unchanged. With the increase of feed per tooth, the surface roughness of nickel-based powder metallurgy superalloy FGH97 changes smoothly first and then increases. When the feed rate of each tooth is between 0.05 mm/z and 0.15 mm/z, the change of surface roughness is not obvious; when the feed rate of each tooth exceeds 0.15 mm/z, the surface roughness of the workpiece increases rapidly. This is because the feed rate is high, the impact force caused by the pore structure of the material itself and the intermittent cutting mode greatly affects the surface quality of the workpiece. The surface roughness is increased. Therefore, considering the actual processing efficiency and other issues, the best feed per tooth is 0.10-0.15mm/z when cutting nickel-base superalloy FGH97.

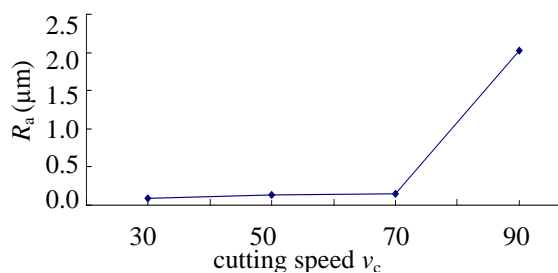


Figure 2. Effect of v_c on surface roughness.

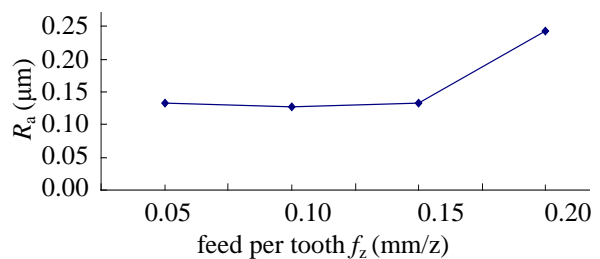


Figure 3. Effect of f_z on surface roughness.

Machined surface roughness corresponding to depth of cut 0.10mm, 0.15mm, 0.20mm and 0.25mm are shown in Figure 4 as cutting speed, feed per tooth and width of cut remaining unchanged.

With the increase of depth of cut, the surface roughness of Ni-base superalloy FGH97 changes smoothly first, then decreases slowly, and finally increases slowly. It can be seen from the diagram that the surface roughness of the workpiece is smaller when the axial cutting depth is between 0.10 mm and 0.20 mm, but in order to ensure the working efficiency of cutting, the cutting depth should be as large as possible without affecting the surface roughness of the workpiece. Therefore, when the depth of cut is between 0.15 mm and 0.20 mm, it can be considered as the most suitable depth of cut for nickel-based powder metallurgy superalloy FGH97.

Machined surface roughness corresponding to width of cut 10mm, 15mm, 20mm and 25mm are shown in Figure 5 as cutting speed, feed per tooth and width of cut remaining unchanged. The effect of width of cut on machined surface roughness is negligible.

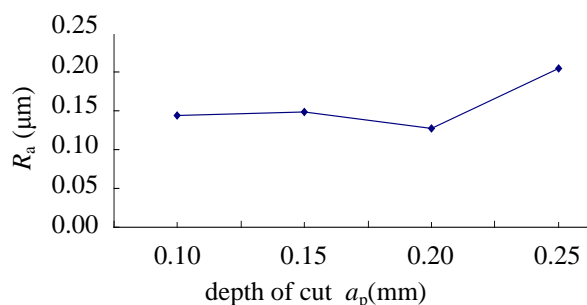


Figure 4. Effect of a_p on surface roughness.

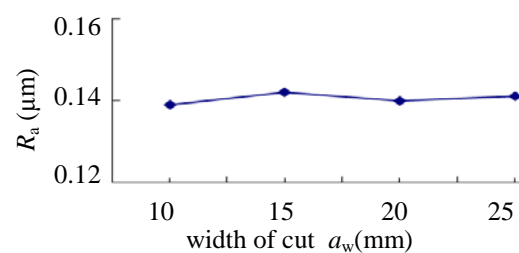


Figure 5. Effect of a_w on surface roughness.

3.3. Roughness Prediction Model

The quadratic models of surface roughness R_a can be established on the basis of measured values shown in Table 4 to observe the effects of individual parameter and the interactions of parameters on the response variables. This kind of models can be written as that shown in Equation (1).

$$Y = a_0 + \sum_{i=1}^4 a_i X_i + \sum_{i=1}^4 a_{ii} X_i^2 + \sum_{i=1}^3 \sum_{j=2, i < j}^4 a_{ij} X_i X_j \quad (1)$$

where Y is the desired responses of R_a . a_0 is a constant. a_i , a_{ii} and a_{ij} represent respectively the coefficients of linear, quadratic and cross-product terms, which identified by fitting the response data using the least square method. X_i corresponds to four cutting parameters.

ANOVA together with F-test were performed on the measured data to identify the significance of each cutting parameter on surface roughness R_a . It follows from Table 4 that F's value for roughness R_a is great larger than the critical value $F_{(0.01)}(4,15)=4.89$. The critical value of linearly dependent coefficient for 99% confidence with 16 degrees of freedom totally in 4 groups $R_{(0.01)}(4,11)$ is 0.8211. The value of R for surface roughness R_a is larger than critical value $R_{(0.01)}(4,11)$. Therefore, the equations (2) for surface roughness calculation is of excellent significance.

$$\begin{aligned} R_a = & -0.0015v_c - 3.1417f_z + 5.9622a_p - 0.0235a_w \\ & + 1.0236 \times 10^{-5} v_c^2 - 2.2161 f_z^2 - 13.2134 a_p^2 + 8.0919 \times 10^{-4} a_w^2 \\ & + 0.0189 v_c f_z + 0.0069 a_p v_c - 2.9021 \times 10^{-5} a_w v_c \\ & + 4.0754 a_p f_z + 0.1572 a_w f_z - 0.1256 a_p a_w - 0.0368 \end{aligned} \quad (2)$$

Table 4. Test of equation signification.

	SS	MS	F	R ²
Model	0.10726	0.00825	29.36175	0.99479

4. Conclusion

The effect of drilling parameters on work hardening and machined surface roughness of nickel-based superalloy FGH97 is summarized according to investigation of its drilling process.

(1) feed rate has a more significant effect on workpiece surface roughness than drilling speed. This is because with the increase of feed, drilling force, machine vibration and workpiece surface roughness increase; with the increase of drilling speed, drilling temperature increases rapidly, workpiece material softens, and its strength and hardness decrease, making the change of workpiece surface roughness smaller.

(2) with the increase of drilling speed, the hardness of workpiece surface is decreasing. When the drilling speed is 10 m/min, the surface hardness of the workpiece reaches the maximum value of 681.6 MPa, while the influence of feed rate on the surface hardness of the workpiece is not significant. With the increase of drilling speed, the depth of workpiece hardening layer becomes smaller and smaller; with the increase of feed, the depth of workpiece hardening layer decreases first and then increases. When the feed rate is 0.07mm/r, the depth of hardened layer reaches a maximum value of 280 μ m.

(3) When TiN/TiAlN coated cemented carbide bits are drilled to process nickel-based superalloys, the wear of the flank is divided into two stages: uniform wear and rapid failure: when the wear of the flank of the bit is less than VB0.16mm, the wear of the flank is more uniform; when the wear of the flank exceeds VB0.16mm, the flank of the bit becomes urgent from the outermost edge to the core of the bit. The wear and tear of the play until the tool fails.

5. Acknowledgments

This work was supported by Shandong Natural Science Foundation of China (No. ZR2017LEE015), Key R & D projects (civil military integration) of Shandong, China.

6. References

- [1] E O Ezugwu, J Bonney, Y Yamane, "An overview of the machinability of aeroengine alloys," *J. Materials Proc. Tech.*, vol. 134, pp.233-253, March 2003.

- [2] C R J Herbert, D A Axinte, M C Hardy, et al, "Investigation into the characteristics of white layers produced in a nickel-based superalloy from drilling operation," *Procedia Engineering*, vol. 19, pp.138-143, 2011.
- [3] Y Liu, Y Ning and Z Yao, et al, "Plastic deformation and dynamic recrystallization of a powder metallurgical nickel-based superalloy," *Journal of Alloys and Compounds*, vol. 675, pp.73-80, August 2016.
- [4] Y Liu, Z Yao and Y Ning, et al, "Effect of deformation temperature and strain rate on dynamic recrystallized grain size of a powder metallurgical nickel-based superalloy," *Journal of Alloys and Compounds*, vol. 691, pp.554-563, January 2017.
- [5] M Zhang, F Li, and Z Yuan, et al, "Effect of heat treatment on the micro-indentation behavior of powder metallurgy nickel based superalloy FGH96," *Materials & Design*, vol. 49, pp.705-715, August 2013.
- [6] M J Zhang, F G Li, S Y Wang and C Y Liu, "Effect of powder reparation technology on the hot deformation behavior of HIPed P/M nickel-base superalloy FGH96," *Materials Science and Engineering: A*, vol. 528, pp. 4030-4039, May 2011.
- [7] B Zhong, Y Wang and D Wei, et al, "Multiaxial fatigue life prediction for powder metallurgy superalloy FGH 96 based on stress gradient effect," *International Journal of Fatigue*, vol. 109, pp. 26-36, April 2018.
- [8] A Devillez, F Schneider and S Dominiak, et al, "Cutting forces and wear in dry machining of Inconel 718 with coated carbide tools," *Wear*, vol. 262, pp.931-942, March 2007.
- [9] Z P Hao, Y H Fan and J Q Lin, et al, "Wear characteristics and wear control method of PVD-coated carbide tool in turning Inconel 718," *The International Journal of Advanced Manufacturing Technology*, vol. 78, pp. 1329-1336, May 2015.
- [10] M C Hardy, C R J Herbert, W Li, et al, "Characterising the integrity of machined surface in a powder nickel alloy used in aircraft engines," *Procedia CIRP*, vol. 13, pp.411-416, 2014.
- [11] A Ginting, M Nouari, "Surface integrity of dry machined titanium alloys," *Int J Mach Tool Manu*, vol. 49, pp.325-332, March 2009.
- [12] J Liu, J Sun and W Chen, "Surface integrity of TB6 titanium alloy after dry milling with solid carbide cutters of different geometriy," *The International Journal of Advanced Manufacturing Technology*, vol. 92, pp. 1-16, October 2017.
- [13] N Varote, SS Joshi, "Microstructure analysis of machined surface integrity in drilling a titanium alloy," *Journal of Materials Engineering and Performance*, vol. 26, pp. 4391-4401, September 2017.
- [14] P J Arrazola, A Kortabarria and A Madariaga, et al, "On the machining induced residual stresses in IN718 nickel-based alloy: experiments and predictions with finite element simulation," *Simulation Modelling Practice and Theory*, vol. 41, pp. 87-103, February 2014.
- [15] T Özel, D Ulutan, "Prediction of machining induced residual stresses in turning of titanium and nickel based alloy with experiments and finite element simulation," *CIRP Annals*, vol. 61, pp.547-550, 2012.
- [16] A Madariaga, P J Arrazola and J A Esnaola, et al, "Evolution of residual stresses induced by machining in a nickel based alloy under static loading at room temperature," *Procedia CIRP*, vol. 13, pp.175-180, 2014.